scientific reports

OPEN

Investigation the behavior of different fullerenes on graphene surface

Mohammad Ali Bakhtiari[1,3], Mohammad Fathi[1,3], Fatemeh Abdolmohammadi[2,3], Seyed Mohammad Ali Hoseinian[1,3], Siavash Sepahi[1,3], Pooya Hooshyar[1,3], Mohammad Taghi Ahmadian[1✉] & Ahmad Assempour[1]

In the present study, the regime of motion of fullerene molecules on graphene substrate in a specific temperature range is investigated. The potential energy of fullerene molecules is analyzed using classical molecular dynamics methods. Fullerene molecules C36, C50, C60, C76, C80, and C90 are selected due to spherical shapes of different sizes and good motion performance in previous studies. Analysis of the motion regime at different temperatures is one of the main objectives of this study. To achieve this aim, the translational and rotational movements of fullerene molecules are studied independently. In the first step of the investigation, Lennard-Jone's potential energy of fullerene molecules is calculated. Subsequently, the motion regime of different fullerenes is classified based on their displacement and diffusion coefficient. Findings indicate C60 is not appropriate in all conditions. However, C90 and C76 molecules are found to be appropriate candidates in most cases in different conditions. As far as a straight-line movement is considered, the deviation of fullerene molecules is compared by their angular velocities. Although C60 has a lower angular velocity due to its symmetrical shape, it may not move well due to its low diffusion coefficient. Overall, our study helps to understand the performance of different fullerene molecules on graphene substrate and find their possible applications, especially as wheels in nanomachine or nanocarrier structures.

Keywords Molecular dynamics, Fullerene, Graphene substrate, Nano carriers, Nanomachines

Natural molecular machines are the core components of the intricate cellular machinery found in living organisms. They perform complex and vital functions, showcasing remarkable efficiency in the transportation of materials[1–3]. The extraordinary capabilities of these biomolecular systems have led to the development of synthetic molecular machines designed to operate at the molecular scale[4,5]. The far-reaching influence of controlled molecular motion on fundamental biological processes confirms the potential benefits that can arise from the advancement of synthetic molecular machines[6–8]. One striking example of these synthetic molecular machines is nanocars, a nanoscale vehicle featuring chassis, axles, and wheels specifically engineered for transportation on various surfaces[9,10]. Development and understanding of molecular motion on surfaces are indispensable in mastering the dynamics and behaviors of molecular machines[5,11]. Among the intriguing questions that have captivated scientists for a considerable time is the intricate relationship between nanomachine design and their diffusion properties[12–14].

A variety of nanomachines, characterized by distinct shapes and differing numbers of wheels, have been developed over time. The first generation of synthetic nanocars featured C60 wheels in their design, marking a pivotal step in the evolution of nanomachine engineering[15,16]. C60, while a well-known molecule, has garnered widespread recognition for its exceptional qualities, as substantiated by numerous experimental and computational studies conducted on diverse substrates[17,18]. Furthermore, the interactions between C60 and substrates like graphene, silicon, and gold have been extensively examined in prior research. Notably, nanocars equipped with fullerene wheels have demonstrated remarkable performance on gold substrates, owing to the combination of their stability and electrical conductivity. Variants of nanomachines, such as four-wheeled and three-wheeled configurations utilizing C60 as wheels, have been previously investigated[19,20].

[1]School of Mechanical Engineering, Sharif University of Technology, Azadi Ave., Tehran, Iran. [2]Department of Chemistry, K.N. Toosi University of Technology, Tehran, Iran. [3]These authors contributed equally: Mohammad Ali Bakhtiari, Mohammad Fathi, Fatemeh Abdolmohammadi, Seyed Mohammad Ali Hoseinian, Siavash Sepahi and Pooya Hooshyar. ✉email: ahmadian@sharif.edu

Significant advancements in this field were made by Vaezi et al.[21], who meticulously explored the motion of C60 molecules on boron nitride substrates at varying temperatures. Their investigation unveiled a transition from dodging to rolling movements as temperatures increased, substantially amplifying the variability of kinetic and diffusion coefficients. Despite the advances made in C60-related research, there is a noteworthy gap in our understanding of the motility regimes of various fullerene molecules on diverse substrates. Consequently, it becomes imperative to assess the applicability and performance of different fullerene molecules on substrates of varying compositions and properties.

In this context, the study conducted by Wang et al.[22] deserves attention, as it investigated the behavior of fullerene molecules, including C60, C72, C180, C240, and C260, on graphene substrates. Notably, each molecule reached the substrate's apex at the swiftest velocity, where their behavior exhibited an intriguing restlessness. These findings have far-reaching implications, as these molecules can potentially be harnessed for the development of high-frequency nano-switches, nanoparticle transport systems, and nanorobotic elements, further showcasing the diverse applications of nanomachines in cutting-edge nanotechnology.

In the last decade, carbon-based materials, including multilayer graphene, graphene, carbon nanotubes, and graphene nanoribbons, have received significant attention for their exceptional electronic and structural properties. These materials have emerged as highly promising candidates for a wide range of applications across various scientific domains such as Nano Sensors, Nano careers, Nano Catalysts, etc.[23–25].

Graphene, in particular, has stood out as a particularly apt substrate for propelling nanocars in nanoscale molecular transport applications, underlining the versatile nature of these carbon-based materials[26].

The recognition of these potential applications has recently highlighted research on the behavior of nanocars on the surfaces of carbon-based materials. Among these investigations, Ejtehadi et al.[19] conducted a detailed examination of the diffusional motion of C60 molecules on graphene substrates. Their study also delved into the effects of these diffusional processes on the integrity of the graphene structure, offering valuable insights into the intricate interactions between nanocars and carbon-based substrates.

Recent exploration highlights the remarkable interplay between nanocars and carbon-based materials, by which there exists a high potential for these materials to advance the field of nanoscale molecular transport and encourage further exploration of their applications in various scientific and technological domains.

Savin et al.[27] studied the thermally induced diffusion of fullerenes on graphene nanoribbons, offering a comprehensive examination of the dynamics governing the interaction between fullerenes and these specialized carbon-based structures. In another study, Jafary-Zadeh et al.[28] devised transport pathways on graphene substrates to restrict the diffusional motion of C60 molecules, introducing a novel approach for fine-tuning and controlling the movement of nanocars on graphene surfaces.

Meanwhile, Ganji et al.[29] employed target density theory to analyze the theoretical exploration of the motion of graphene and nanocars equipped with p-carborane wheels on graphene surfaces. Their theoretical investigation provides valuable insights into the dynamic behavior of nanocars and the underlying principles governing their mobility on graphene surfaces. This innovative approach bridges the gap between theory and practical applications, offering a promising approach for the further advancement of nanocar technology. These collective efforts underline the vibrant and multifaceted research focused on understanding and harnessing the potential of nanocars on graphene substrates.

Monolayers and few-layers of graphene, while often portrayed as perfectly flat, actually exhibit a characteristic wavy morphology on their surfaces, characterized by ripples and out-of-plane deformations[30]. Scanning tunneling microscopy (STM) has offered a fascinating glimpse into the intricate world of graphene, unveiling the presence of thermally induced ripples that traverse through this two-dimensional lattice in the form of standing waves. These ripple waves, captivating in their erratic evolution, possess the potential to exert a profound influence on the motion of nanocars[31]. The intermittent variations in the contact level and the intricate interlock effects generated by these graphene ripples can introduce an element of unpredictability into the otherwise finely orchestrated dance of molecule translation.

While prior research has contributed to our understanding of the dynamics of a single molecule, such as C60, on flat graphene surfaces, surprisingly, the intricate dynamics of nanocars moving across flexible graphene surfaces along with ripples need to be explored[21,30]. The lack of such investigations leaves a conspicuous gap in our comprehension of how these remarkable nanomachines navigate the undulating of graphene. In addition to the ripple-induced uncertainties, another intriguing facet awaiting exploration is the role of chassis rigidity in the surface dynamics of nanomachines. To the best of our knowledge, no previous studies have ventured into the uncharted terrain been conducted on nanomachines as they gracefully maneuver across the graphene substrate, where ripples and rigidity combine to craft an unexplored and captivating choreography of molecular transport.

In the present study, we have investigated the intricate interplay between fullerene size and temperature variations and their impact on the migration of fullerenes. To achieve this goal, we have conducted a comprehensive examination of the motion of several fullerene molecules on a graphene substrate. Specifically, we have selected C36, C50, C60, C76, C80, and C90 fullerene molecules, each distinguished by its spherical shape and varying size.

The first phase of our investigation involved the calculation of the potential energy for these fullerene molecules. This preliminary step provided invaluable insights into the energy level governing fullerene movement. Based on the obtained results, we projected the likely trajectories and behaviors of fullerenes under different conditions.

Furthermore, we employed the classical molecular dynamics method to examine the motion of fullerenes. Importantly, we conducted these simulations on thermally induced substrates, enabling us to gain better control over fullerene movement and to replicate real-world conditions more accurately.

The modeling of fullerene motion accomplished in this study holds profound implications. It serves as a critical foundation for foreseeing and manipulating the movements of fullerene-based nanocars across a wide spectrum of potential applications. This comprehensive exploration of the dynamic behavior of fullerenes on

graphene substrates advances our understanding of these molecular systems and sets the stage for groundbreaking developments in nanocar technology.

Methods
Potential energy of fullerenes

The estimation of potential energy proves to be a highly effective method for the anticipation of fullerene mobility on a variety of substrates. In this section, a comprehensive investigation is performed on the mobility of multiple fullerenes, as depicted in Fig. 1, on the graphene substrate, illustrated in Fig. 2.

It is crucial to emphasize that during the computation of potential energy, the fullerene molecule' bonds is considered to be rigid to improving the time step of simulations[32–34]. The molecular structures of all fullerenes are provided by the Nanotube Modeler program in the fullerene library[35]. Some fullerene molecules have many isomers, so we select the one that has a spherical shape like C60 (e.g. From the nanotube modeler, we selected specific isomers based on their spherical shapes: No.15-D6h.cc1 from the 15 isomers of C36, No.271-D5h.cc1 from the 271 isomers of C50, C76-Td.cc1 from the 2 isomers of C76, No.6-D5h.cc1 from the 7 isomers of C80, and No.20-C1.cc1 from the 46 isomers of C90).

A study by Pishkenari et al.[36] shows that the potential energy of C60 on a gold substrate exhibits variation contingent upon its orientation. Their study encompassed an examination of four distinct C60 orientations, accounting for both translational and rotational motions, ultimately discerning that the Hexa-down orientation stands as the most stable configuration for motion[33,36]. Consequently, in the current study, the Hexa-down orientation is consistently adopted for all the aforementioned fullerenes, establishing a uniform and stable foundation for the investigation of their mobility on the graphene substrate. This deliberate choice streamlines the analysis and allows for meaningful comparisons across various fullerenes.
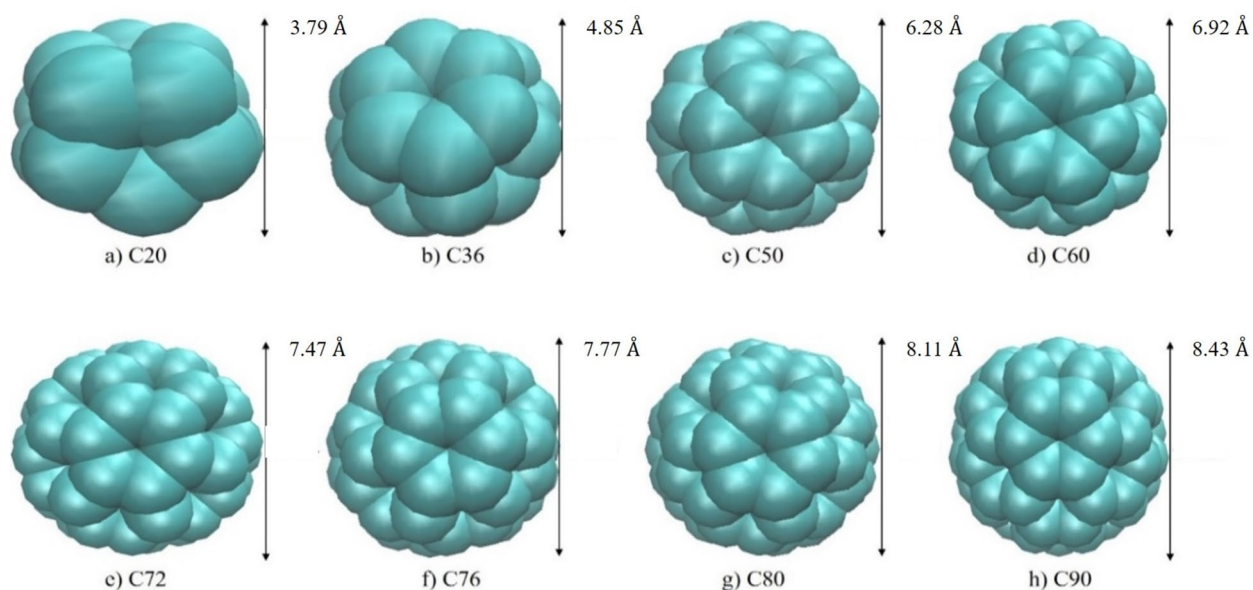

Figure 1. Different fullerenes with their diameters simulated in this paper are C20 (**a**), C36 (**b**), C50 (**c**), C60 (**d**), C72 (**e**), C76 (**f**), C80 (**g**) and C90 (**h**).
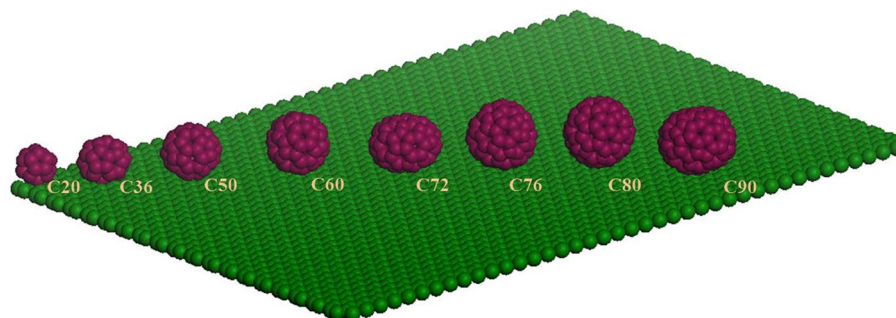

Figure 2. The fullerene molecules contacted from Hexa-Down orientation on the graphene surface.

Tersoff potential is used to calculate bonded terms in graphene and fullerenes (except covalent bond for fullerenes). Lennard–Jones 6–12 (LJ6-12) potential is used to describe the non-bonded interaction between each atom of graphene with each atom of fullerenes, which is expressed as follows (Eq. 1):

$$E_{Lj} = 4\varepsilon \left[\left(\frac{\sigma}{r} \right)^{12} - \left(\frac{\sigma}{r} \right)^{6} \right]. \tag{1}$$

In this equation, the terms σ, ε, and r represent the crucial potential parameters governing the interaction between the carbon atoms. Specifically, σ denotes the equilibrium distance of the C–C bond, and it is set σ =3.4 Angstroms (Å). The parameter ε designates the well depth of the potential with a value of ε =2.41 milli-electronvolts (meV)[21,30,33,37]. The parameter r is the distance between the carbon atoms of the fullerene and the carbon atoms constituting the graphene substrate at an equilibrium position.

Furthermore, $r_{cut-off}$ stands as the cut-off radius for the Lennard–Jones potential and is defined as $r_{cut-off}$ = 13.5 Angstroms (Å). This value serves to delimit the range over which the Lennard–Jones potential influences the interaction between the fullerene and the graphene substrate. The application of the Lennard–Jones potential with these specific parameters facilitates a precise estimation of potential energy, forming the cornerstone of our investigation into the mobility of fullerenes on the graphene substrate[30,37].

Simulation setup

In the present study, the motion of several fullerene molecules on the graphene surfaces has been analyzed using the classic molecular dynamics method. The substrates are modeled as 12×12 nm^2 square sheets containing 5744 carbon atoms based on the previous works[37]. Additionally, periodic boundary conditions were utilized in the x and y directions. The flat graphene sheet is positioned at $z=0$ plane. Simulations are accomplished at different temperatures in the range of 75 to 600K to investigate the effect of the temperature on the behavior of fullerene molecules. The temperature of the substrate and fullerenes is controlled by employing the Nose–Hoover thermostat[38]. The fullerene molecule is placed on top of the substrate.

Simulations are performed using Large-scale Atomic/Molecular Massively Parallel Simulator)LAMMPS(software[39] (https://www.lammps.org/), and the results are envisioned utilizing the Visual Molecular Dynamics (VMD) package[40] (http://www.ks.uiuc.edu/Research/vmd/). Before starting the simulation, the system is relaxed for 250,000 steps, and then the simulation is performed for 8 ns considering 1 fs time step to attain accurate results. The velocity Verlet algorithm is utilized to integrate the equations of motion with a 1 fs time step. T_{damp} set to 50 fs in the LAMMPS software for NVT ensemble as well[41].

Results and discussion

Historically, research predominantly centered on the C60 fullerene molecule, with less attention given to other fullerene variants. Meanwhile, the use of other carbon nanoparticles, such as graphene sheets, has gained substantial popularity in recent studies.

In the present investigation, we not only explore C60 fullerenes but also simulate other fullerene structures on a graphene substrate. This innovative approach allows us to observe the influence of altering the radius of fullerene molecules in conjunction with temperature variations on a graphene surface.

Figure 3 illustrates the motion of each of these fullerene molecules on the graphene surface. This study involves simulations conducted at three distinct temperature ranges: 75 and 150 K (degrees Kelvin) as the low-temperature range, 300 and 400 K as the intermediate-temperature range, and two additional temperatures of 500 K and 600 K within the high-temperature range.

The analysis of Fig. 3A and B reveals that at lower temperatures, the C90 fullerene molecule demonstrates the most effective performance. In this context, within this temperature range, the dominant mode of motion is molecular sliding, and lateral motion is not observed. The larger number of molecules in the C90 molecule enables it to exhibit superior motion performance in this specific temperature range.

An essential observation within this temperature range is the limited movement of the C60 molecule, which is traditionally the primary focus of fullerene studies. In contrast, other molecules, such as C90, C76, C50, and C36, have consistently exhibited more favorable motion behavior than the C60 molecule. This trend persists as the temperature rises into the intermediate temperature range. At temperatures of 300 K and 400 K, molecules like C76 and C50 continue to demonstrate highly desirable performance, as evident in Fig. 3C and D.

At 300 K, it is noted that the C90 molecule does not exhibit the best performance among fullerene molecules. This can be attributed to the prevalence of rolling motion over sliding motion for these molecules. Given its greater mass, the rolling motion of the C90 molecule is more demanding and necessitates a higher energy input. Raising the temperature to 400 K and thus supplying the required energy to facilitate the rolling motion of the C90 molecule enhances its performance.

In the case of other molecules, especially the smaller ones, substantial deviations in motion are noticeable, as rolling is considerably straightforward for them. As the temperature rises, entering the high-temperature range (500 and 600 K), a range of molecules display improved long-range movements. Apart from a limited number of direct linear movements, the predominant mode of motion transitions to rotational movements around themselves within the hexagonal lattice, as depicted in Fig. 3E and F.

To delve into the finer nuances of these molecules' behavior, a range of motion-related parameters, including displacement, velocity, diffusion coefficient, and etc. are analyzed. These parameters will offer a more comprehensive understanding of the motion of these molecules.

The initial investigated parameter is the distance traveled by various fullerenes, and the results are presented in Fig. 4. It is evident that, as the temperature rises, all molecules travel significantly greater distances. Additionally,
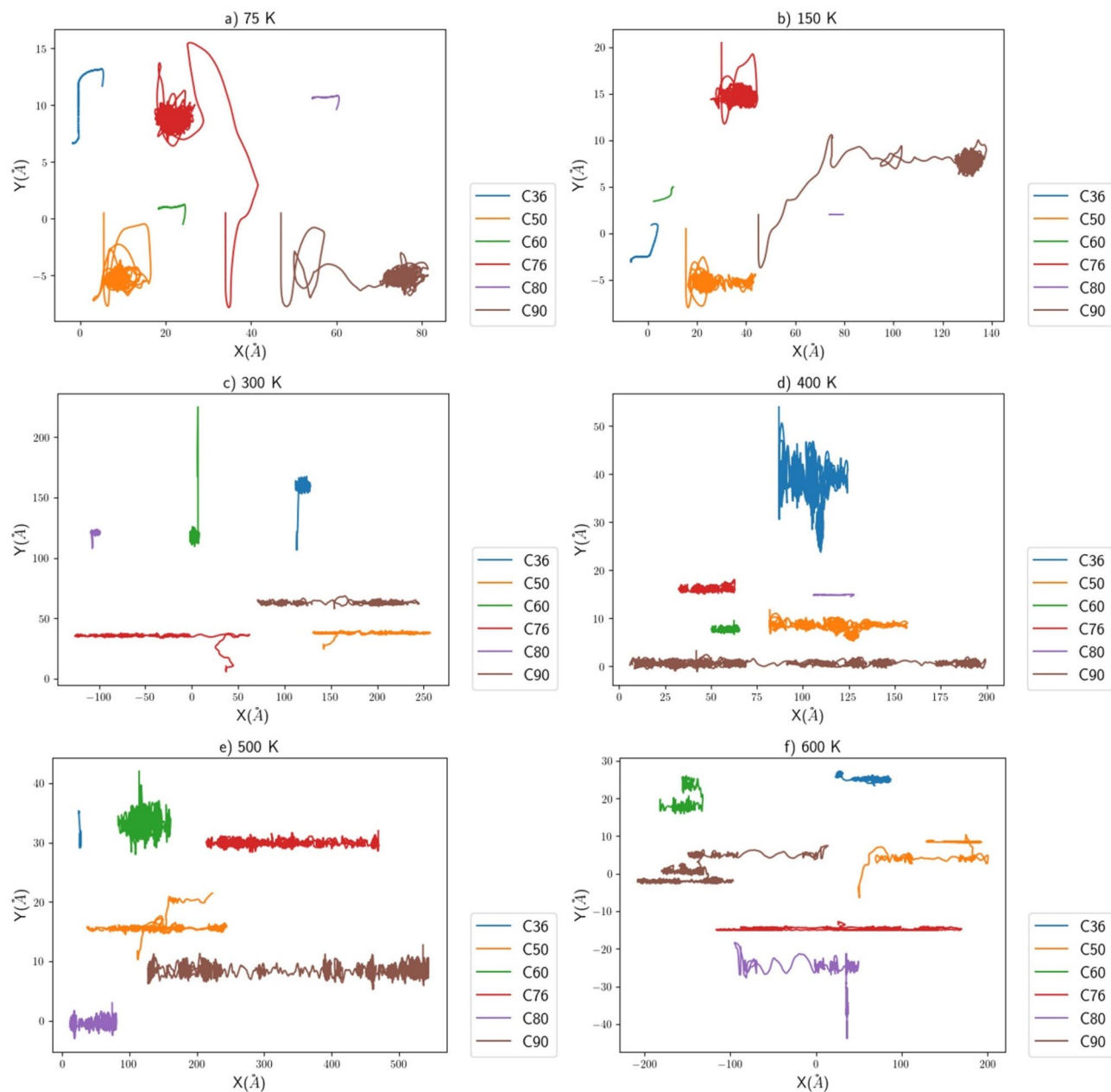
Figure 3. Comparison of trajectories of fullerene molecules at the temperatures of (**a**) 75 K, (**b**) 150 K, (**c**) 300 K, (**d**) 400 K, (**e**) 500 K and (**f**) 600K on graphene substrate.

we observe the impact of molecular size on the distance traveled by fullerenes at a given temperature. In essence, as the size of the fullerene increases, the distance it travels under the same conditions also increases. This phenomenon is attributed to the larger number of carbon atoms in the molecule, resulting in increased interaction with the surface and, consequently, longer distances traveled.

Upon examining the displacement of each fullerene, it becomes evident that the size of the fullerene has minimal influence on their displacement. Figure 5 illustrates significant differences in displacement across various conditions. In nearly all cases, the C90 fullerene has displayed favorable performance. To gain a deeper understanding of the underlying reasons for this observation, it is essential to analyze and assess other behavioral parameters of fullerenes. This includes parameters that influence motion, such as the diffusion coefficient, as well as parameters affecting deviations in motion, like angular velocity and effective velocity of the fullerenes (The types of fullerene molecules motion have been provided in Table S1).

Figure 6 displays the diffusion coefficients of fullerenes under various conditions. Upon analyzing the trend of changes in the chart and its correlation with Fig. 5, it is clear that higher displacement is linked to higher diffusion coefficients. Another important observation from this chart is the consistently low diffusion coefficient of the C60 molecule, as it never attained the highest value in any scenario.
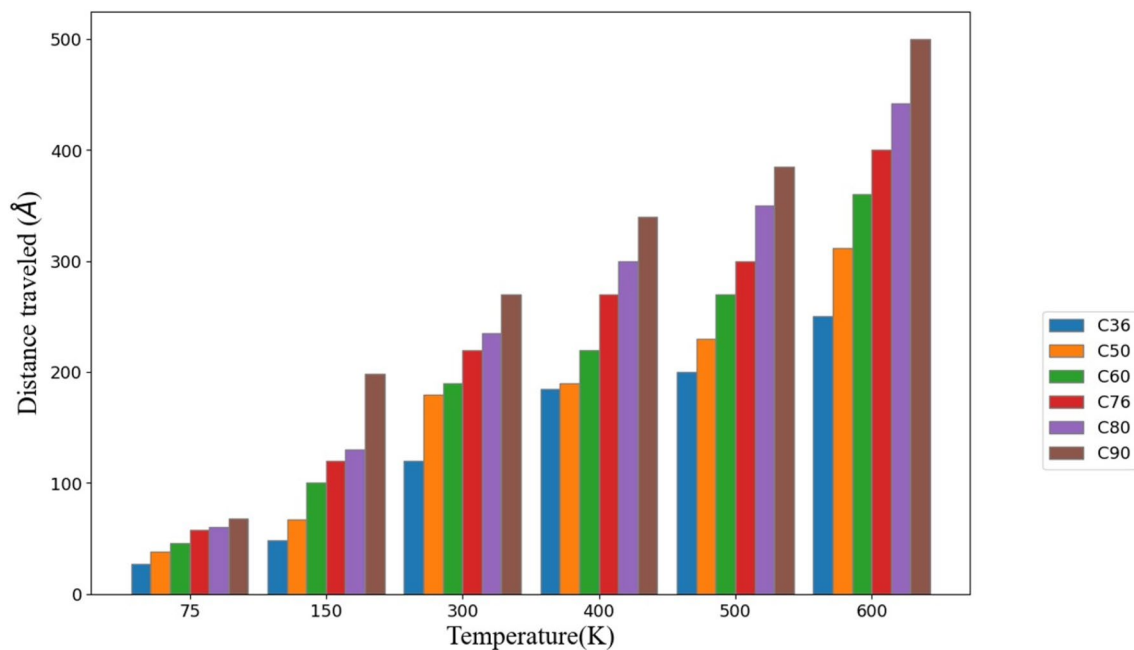
Figure 4. Comparison of the distance traveled by fullerene molecules at different temperatures.
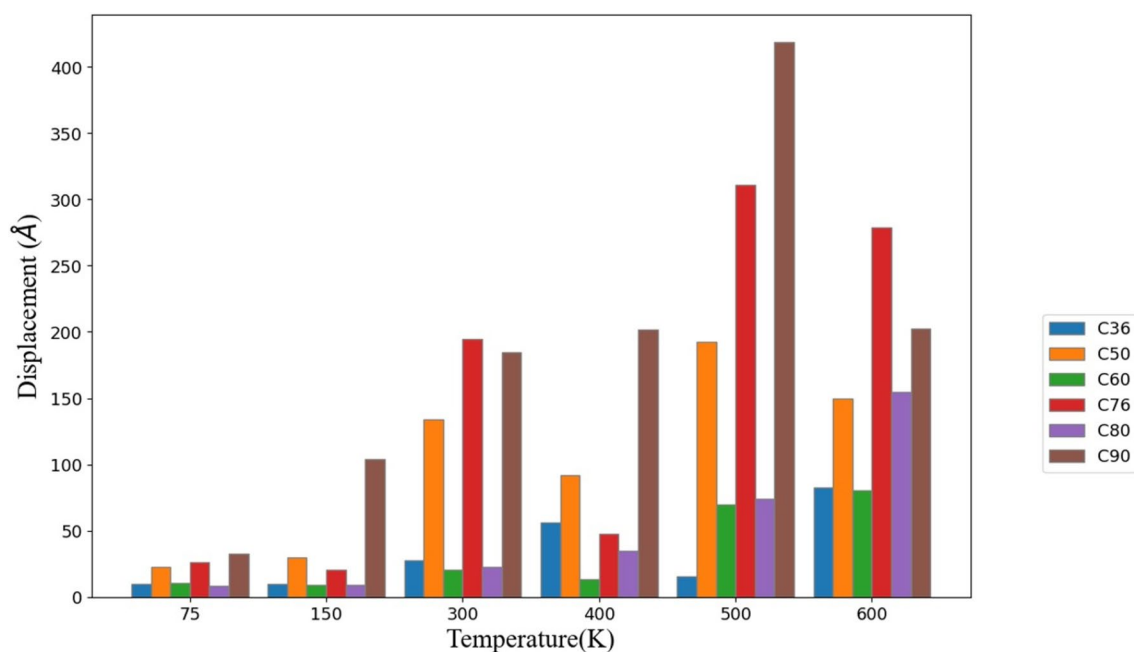

Figure 5. Comparison of the displacement of fullerene molecules at different temperatures.

An additional noteworthy observation from the figure is that it signifies the occurrence of long-range motion for fullerenes in nearly all cases. In prior studies, a diffusion coefficient of 0.01 was emphasized as the minimum requirement for transitioning from short-range to long-range motion[34]. In this simulation, this minimum value is observed in almost all instances, underscoring the suitability of carbon surfaces, such as graphene, for facilitating the motion of these molecules.

For a more comprehensive comprehension of the performance of different fullerenes, it is crucial to consider parameters related to deviations in molecular motion. In this study, an analysis of two key parameters, namely effective velocity (Fig. 7) and angular velocity perpendicular to motion (Fig. 8), has been conducted to provide further insights.

The effective velocity of a molecule, in essence, signifies the molecule's velocity in the expected direction relative to the molecule's overall velocity. As depicted in Fig. 7, it is evident that most molecules with substantial
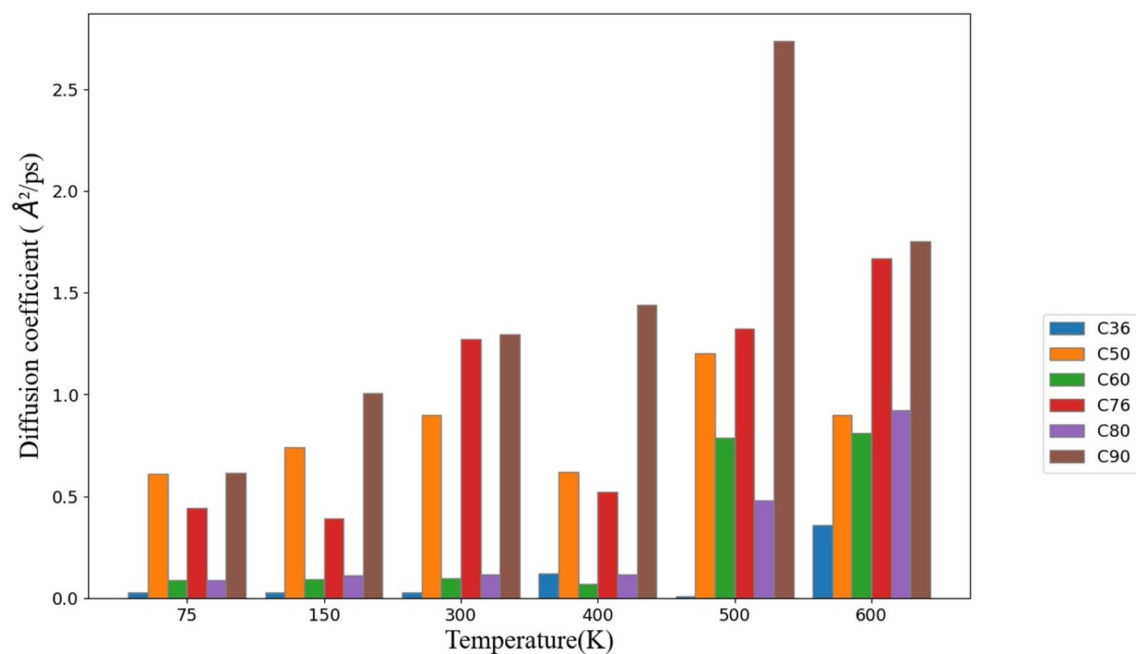
Figure 6. Comparison of the diffusion coefficient of fullerene molecules at different temperatures.
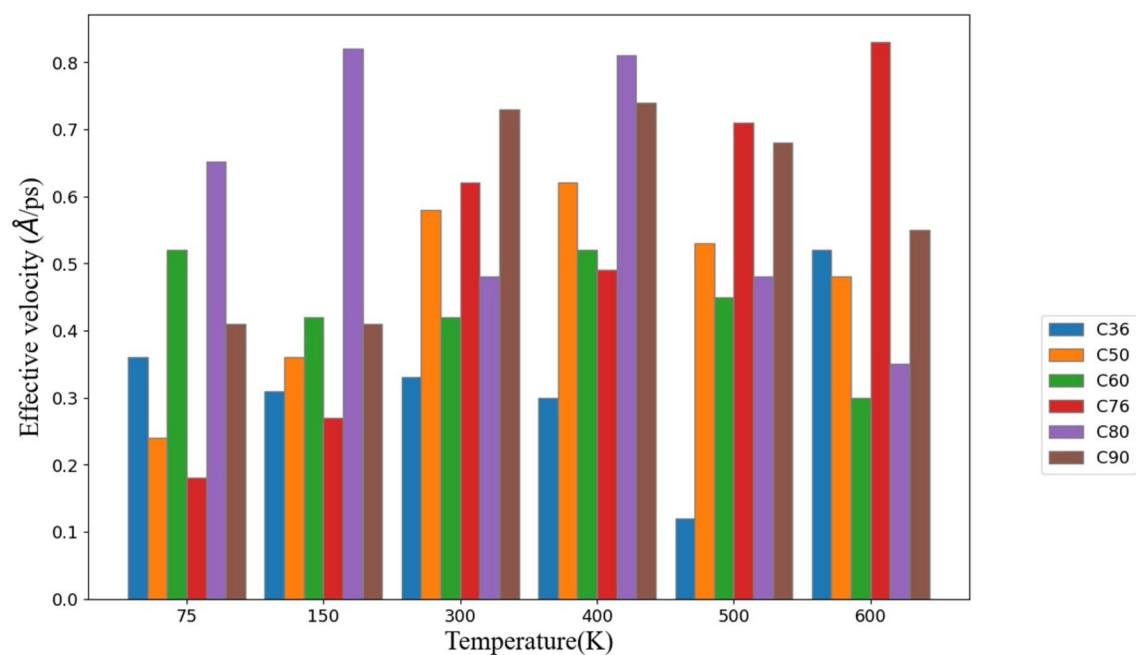

Figure 7. Comparison of the effective velocity of fullerene molecules at different temperatures.

displacements exhibit higher effective velocities. However, observation indicates that certain molecules, like the C80 molecule at 150 K, experienced a reduction of over 80% in their effective velocity. This phenomenon is attributed to the fluctuating motion of the molecule, which can be rationalized considering the observed displacement and the relatively high diffusion coefficient of the molecule, as illustrated in Figs. 3B and 4.

Another insightful parameter that effectively serves as an indicator of deviation in fullerene molecules is the angular velocity of the molecule in the direction perpendicular to the motion, particularly along the z-axis in this research. This parameter provides valuable insights into the extent to which molecules have deviated from their primary path during motion.

Upon examining Fig. 8, it becomes apparent that the C60 molecule, despite the challenges discussed in various sections, has experienced the least deviation in the direction of its symmetrical shape. This molecule consistently
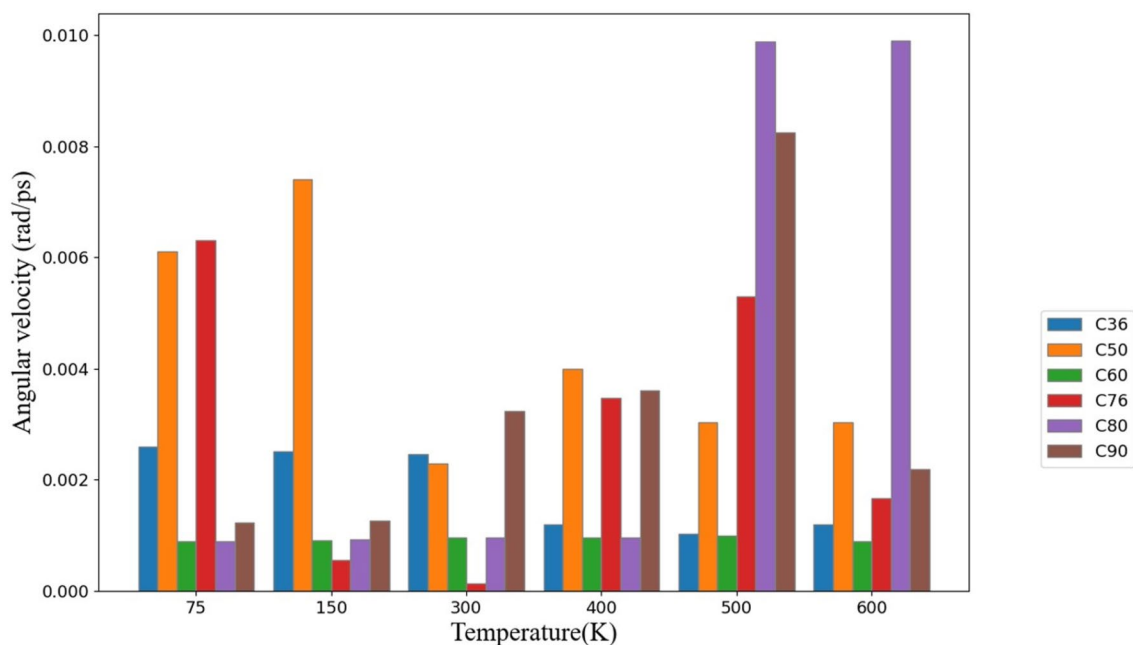
Figure 8. Comparison of the angular velocity of fullerene molecules at different temperatures.

exhibits the lowest angular velocity. Consequently, it can be inferred that the primary issue with this molecule is its low diffusion coefficient, as previously discussed.

By examining all the intricacies of the motion behavior of these molecules and taking into account the obtained results in various sections, it is evident that this study effectively addresses a crucial aspect in nano machines and carbon-based mobile molecules. In summary, it can be deduced that, by consulting Tables 1 and 2, we can make more informed choices than relying solely on the C60 fullerene. The appropriate fullerene for each temperature and the overall ranking of fullerenes based on their overall performance can be determined from the findings of this study.

According to Table 1 and considering that sliding motion is the best type of motion for the molecule, in the low-temperature range such as 75 and 150 K, larger fullerenes exhibit sliding motion, while smaller fullerenes gradually experience interference between rolling and sliding motions as the temperature increases. This phenomenon has caused greater deviations for them. Additionally, at a temperature of 75 K, larger fullerenes such as C80 and C90 could not exhibit reasonable movement due to the resistance from their higher inertia. Consequently, C76, with its lower inertia, exhibited better movement. With the increase in temperature up to 150

Temperature	Fullerene
75	C76
150	C90
300	C50
400	C90
500	C90
600	C76

Table 1. Candidate fullerenes in different temperatures.

Place	Fullerenes
1	C90
2	C76
3	C50
4	C80
5	C60
6	C36

Table 2. Fullerenes' ranks based on their performance on the graphene substrate.

K and with larger fullerenes such as C90 overcoming their inertia and creating sliding motion, these fullerenes have been able to exhibit better movement. With the increase in temperature, the interference between sliding and rolling motion will shift from smaller fullerenes to larger ones. In smaller fullerenes, rolling motion will gradually dominate over sliding, resulting in fewer deviations in their movement. Therefore, as the temperature rises to 300 K, it will be the larger fullerenes that experience interference between sliding and rolling motions. Consequently, lighter fullerenes such as C50, where rolling motion dominates over sliding as previously mentioned, will exhibit better movement. As the temperature increases to 400 K and then 500 K, and with rolling motion dominating over sliding in larger fullerenes such as C90, we will once again observe better performance from the larger fullerenes. Finally, at a temperature of 600 K, due to the excessively high temperature, C76, which slightly deviates from structural symmetry, performs better because this asymmetry allows it to move more efficiently in one direction.

According to Table 2, it can be stated that heavier fullerenes have performed better compared to lighter fullerenes. Among factors such as molecular symmetry and size, one of the significant factors influencing the performance of heavier fullerenes is their weight. Due to this weight and their closer energy absorption to the graphene surface, they naturally exhibit better movement. This is in accordance with the Lennard–Jones potential (Eq. 1), where reduced distance (r) results in higher energy and consequently better movement.

According to Table 2, it is evident that other fullerenes, which have not been significantly studied or considered so far, can perform better for applications that have traditionally used C60 fullerene. Based on the data in this table, C60 fullerene does not appear in the top positions, suggesting that these other fullerenes may offer superior performance for such applications.

Conclusion

The use of carbon-based nanoparticles has surged recently across various applications[33,34,42], encompassing materials such as fullerenes, graphene sheets, and carbon nanotubes. There is a growing emphasis on nanocarriers and nanomaterials for delivering nanostructures, particularly in pharmaceutical applications. Molecular machines based on fullerenes are notable among these nanocarriers.

Numerical methods have become essential tools for studying nanoparticles due to their precision, speed, and cost-effectiveness[43–45]. This study employs molecular dynamics principles to explore the behavior of different fullerenes on a graphene surface. Unlike previous studies that focused primarily on C60 fullerenes, this research investigates the potential of other fullerenes through simulations.

Additionally, this study examines how altering the size of fullerenes affects their motion on a graphene surface under varying temperatures.

The simulation results indicate a direct relationship among the distance traveled by different fullerenes, temperature variations, and the number of carbon atoms within the fullerene structure. This suggests that as both temperature and the carbon atom count increase, so does the distance traveled by the fullerenes. This effect is attributed to enhanced interactions between fullerenes and the surface, allowing them to engage more effectively and cover longer distances.

Upon examining other critical parameters evaluated in the simulations, it becomes clear that the distance traveled alone cannot solely determine the superior or inferior performance of fullerenes as initially expected. Simply traveling a greater distance does not necessarily indicate better performance. To gain a more comprehensive understanding, it is essential to consider the analysis of additional factors such as the diffusion coefficient and deviation. These factors are crucial in evaluating the overall performance of fullerenes.

The diffusion coefficient quantifies how efficiently a fullerene moves between locations by transferring energy to surrounding molecules. It should be noted that the diffusion coefficient alone cannot be the sole indicator of superior performance for fullerenes that travel longer distances. Even if a fullerene covers a greater distance, its performance may not be better if its diffusion coefficient is low. Therefore, the diffusion coefficient should be assessed alongside other parameters to provide a comprehensive evaluation of a fullerene's performance.

Additionally, parameters related to deviations and angular velocities of molecules are crucial in assessing fullerene performance. Generally, fullerenes with higher effective velocities and lower angular velocities tend to perform better, although there are exceptions. For instance, the C80 fullerene at 150 K, despite traveling further than C60, does not show superior performance due to its low diffusion coefficient and fluctuating motion under specific conditions.

Simulation results indicate a correlation between angular velocity perpendicular to the motion plane and molecule deviation from their primary path. Fullerenes with symmetric structures, such as C60, exhibit less deviation, suggesting symmetry aids in maintaining consistent motion trajectories. However, deviations from the primary path, influenced by factors like diffusion coefficient and angular velocity, impact fullerene performance. Excessive deviation can lead to inefficient motion or stalling, affecting overall molecule performance in nanostructure applications.

In conclusion, this study highlights varied performances among different fullerenes, emphasizing the importance of selecting the appropriate type for specific applications. Performance isn't solely determined by distance traveled; factors like angular velocity and diffusion coefficient significantly influence fullerene behavior and suitability for various applications. Understanding these factors is crucial for optimizing fullerene functionality in practical applications.

Data availability

The data of this study is available upon reasonable request from the corresponding author.

References

1. Lancia, F., Ryabchun, A. & Katsonis, N. Life-like motion driven by artificial molecular machines. *Nat. Rev. Chem.* **3**(9), 536–551 (2019).
2. García-López, V., Liu, D. & Tour, J. M. Light-activated organic molecular motors and their applications. *Chem. Rev.* **120**(1), 79–124. https://doi.org/10.1021/acs.chemrev.9b00221 (2020).
3. Mavroidis, C., Dubey, A. & Yarmush, M. L. Molecular machines. *Annu. Rev. Biomed. Eng.* **6**(1), 363–395. https://doi.org/10.1146/annurev.bioeng.6.040803.140143 (2004).
4. Bustamante, C., Macosko, J. C. & Wuite, G. J. Grabbing the cat by the tail: Manipulating molecules one by one. *Nat. Rev. Mol. Cell Biol.* **1**(2), 130–136 (2000).
5. Baroncini, M. *et al.* Making and operating molecular machines: A multidisciplinary challenge. *ChemistryOpen* **7**(2), 169–179. https://doi.org/10.1002/open.201700181 (2018).
6. Balzani, V., Credi, A. & Venturi, M. The bottom-up approach to molecular-level devices and machines. *Chem. Eur. J.* **8**(24), 5524–5532. https://doi.org/10.1002/1521-3765(20021216)8:24%3c5524::AID-CHEM5524%3e3.0.CO;2-J (2002).
7. Balzani, V., Credi, A. & Venturi, M. Molecular-level devices. In *Supramolecular Science: Where It Is and Where It Is Going* (eds Ungaro, R. & Dalcanale, E.) 1–22 (Springer, Netherlands, 1999). https://doi.org/10.1007/978-94-011-4554-1_1.
8. Kay, E. R., Leigh, D. A. & Zerbetto, F. Synthetic molecular motors and mechanical machines. *Angew. Chem. Int. Ed.* **46**(1–2), 72–191 (2007).
9. Shirai, Y., Osgood, A. J., Zhao, Y., Kelly, K. F. & Tour, J. M. Directional control in thermally driven single-molecule nanocars. *Nano Lett.* **5**(11), 2330–2334. https://doi.org/10.1021/nl051915k (2005).
10. Kudernac, T. *et al.* Electrically driven directional motion of a four-wheeled molecule on a metal surface. *Nature* **479**(7372), 208–211. https://doi.org/10.1038/nature10587 (2011).
11. Baroncini, M., Silvi, S. & Credi, A. Photo- and redox-driven artificial molecular motors. *Chem. Rev.* **120**(1), 200–268. https://doi.org/10.1021/acs.chemrev.9b00291 (2020).
12. Rapenne, G. & Joachim, C. The first nanocar race. *Nat. Rev. Mater.* **2**(6), 1–3 (2017).
13. Pawlak, R. & Meier, T. Fast and curious. *Nat. Nanotechnol.* **12**(7), 712–712 (2017).
14. Pawlak, R. *et al.* Design and characterization of an electrically powered single molecule on gold. *ACS Nano* **11**(10), 9930–9940 (2017).
15. Morin, J.-F., Sasaki, T., Shirai, Y., Guerrero, J. M. & Tour, J. M. Synthetic routes toward carborane-wheeled nanocars. *J. Org. Chem.* **72**(25), 9481–9490. https://doi.org/10.1021/jo701400t (2007).
16. Lohrasebi, A., Neek-Amal, M. & Ejtehadi, M. R. Directed motion of C 60 on a graphene sheet subjected to a temperature gradient. *Phys. Rev. E* **83**(4), 042601. https://doi.org/10.1103/PhysRevE.83.042601 (2011).
17. Neek-Amal, M., Abedpour, N., Rasuli, S. N., Naji, A. & Ejtehadi, M. R. Diffusive motion of C 60 on a graphene sheet. *Phys. Rev. E* **82**(5), 051605. https://doi.org/10.1103/PhysRevE.82.051605 (2010).
18. Cuberes, M. T., Schlittler, R. R. & Gimzewski, J. K. Room-temperature repositioning of individual C60 molecules at Cu steps: Operation of a molecular counting device. *Appl. Phys. Lett.* **69**(20), 3016–3018. https://doi.org/10.1063/1.116824 (1996).
19. Ozmaian, M., Fathizadeh, A., Jalalvand, M., Ejtehadi, M. R. & Allaei, S. M. V. Diffusion and self-assembly of C 60 molecules on monolayer graphyne sheets. *Sci. Rep.* **6**(1), 21910 (2016).
20. Martsinovich, N. & Kantorovich, L. Modelling the manipulation of C60 on the Si (001) surface performed with NC-AFM. *Nanotechnology* **20**(13), 135706 (2009).
21. Vaezi, M., Nejat Pishkenari, H. & Nemati, A. Mechanism of C60 rotation and translation on hexagonal boron-nitride monolayer. *J. Chem. Phys.* https://doi.org/10.1063/5.0029490 (2020).
22. Wang, L. & Xu, Z. A graphene-based nanoparticle motion converter. *Int. Core J. Eng.* **5**(1), 114–118 (2019).
23. Kazemzadeh, H. & Mozafari, M. Fullerene-based delivery systems. *Drug Discov. Today* **24**(3), 898–905. https://doi.org/10.1016/j.drudis.2019.01.013 (2019).
24. Seifi, S. *et al.* Engineering biomimetic scaffolds for bone regeneration: Chitosan/alginate/polyvinyl alcohol-based double-network hydrogels with carbon nanomaterials. *Carbohydr. Polym.* **339**, 122232. https://doi.org/10.1016/j.carbpol.2024.122232 (2024).
25. Azizpour, R., Zakeri, H. & Moradi, G. Beam pattern control for graphene-based patch array antenna with radio-over-fiber systems by using modulation instability phenomenon. *Opt. Contin.* **2**(4), 865–876 (2023).
26. Meyer, J. C. *et al.* The structure of suspended graphene sheets. *Nature* **446**(7131), 60–63 (2007).
27. Savin, A. V. & Kivshar, Y. S. Transport of fullerene molecules along graphene nanoribbons. *Sci. Rep.* **2**(1), 1012 (2012).
28. Jafary-Zadeh, M. & Zhang, Y.-W. Molecular mobility on graphene nanoroads. *Sci. Rep.* **5**(1), 12848 (2015).
29. Ganji, M. D., Ahangari, M. G. & Emami, S. M. Carborane-wheeled nanocar moving on graphene/graphyne surfaces: Van der Waals corrected density functional theory study. *Mater. Chem. Phys.* **148**(1–2), 435–443 (2014).
30. Vaezi, M., Nejat Pishkenari, H. & Ejtehadi, M. R. Programmable transport of C60 by straining graphene substrate. *Langmuir* **39**(12), 4483–4494. https://doi.org/10.1021/acs.langmuir.3c00180 (2023).
31. Grill, L. ChemInform abstract: Functionalized molecules studied by STM: Motion, switching and reactivity. *ChemInform* https://doi.org/10.1002/chin.200823260 (2008).
32. Alireza, N., Meghdari, A., Nejat Pishkenari, H. & Sohrabpour, S. Investigation into thermally activated migration of fullerene-based nanocars. *Sci. Iran.* https://doi.org/10.24200/SCI.2018.20321 (2018).
33. Shamloo, A., Bakhtiari, M. A., Tohidloo, M. & Seifi, S. Investigation of fullerene motion on thermally activated gold substrates with different shapes. *Sci. Rep.* **12**(1), 14397. https://doi.org/10.1038/s41598-022-18730-7 (2022).
34. Bakhtiari, M. A., Seifi, S., Tohidloo, M. & Shamloo, A. Investigation of the motion of fullerene-wheeled nano-machines on thermally activated curved gold substrates. *Sci. Rep.* **12**(1), 18255. https://doi.org/10.1038/s41598-022-22517-1 (2022).
35. Asadollahi, D. & Shariati, M. Investigation of shear forces in twisted carbon nanotube bundles using a structural mechanics approach. *Acta Mech.* **232**(6), 2425–2441. https://doi.org/10.1007/s00707-021-02949-y (2021).
36. Nejat Pishkenari, H., Nemati, A., Meghdari, A. & Sohrabpour, S. A close look at the motion of C60 on gold. *Curr. Appl. Phys.* **15**(11), 1402–1411. https://doi.org/10.1016/j.cap.2015.08.003 (2015).
37. Mofidi, S. M., Nejat Pishkenari, H., Ejtehadi, M. R. & Akimov, A. V. Locomotion of the C60-based nanomachines on graphene surfaces. *Sci. Rep.* **11**(1), 2576. https://doi.org/10.1038/s41598-021-82280-7 (2021).
38. Martyna, G. J., Klein, M. L. & Tuckerman, M. Nosé–Hoover chains: The canonical ensemble via continuous dynamics. *J. Chem. Phys.* **97**(4), 2635–2643. https://doi.org/10.1063/1.463940 (1992).
39. Plimpton, S. Fast parallel algorithms for short-range molecular dynamics. *J. Comput. Phys.* **117**(1), 1–19. https://doi.org/10.1006/jcph.1995.1039 (1995).
40. Humphrey, W., Dalke, A. & Schulten, K. VMD: Visual molecular dynamics. *J. Mol. Graph.* **14**(1), 33–38. https://doi.org/10.1016/0263-7855(96)00018-5 (1996).

41. Yu, T.-Q., Alejandre, J., López-Rendón, R., Martyna, G. J. & Tuckerman, M. E. Measure-preserving integrators for molecular dynamics in the isothermal–isobaric ensemble derived from the Liouville operator. *Chem. Phys.* **370**(1–3), 294–305. https://doi.org/10.1016/j.chemphys.2010.02.014 (2010).
42. Bakhtiari, M. A. *et al.* Effects of different wheels on the mobility of thermally driven fullerenes-based nanotrucks. *Sens. Actuators Phys.* **363**, 114769. https://doi.org/10.1016/j.sna.2023.114769 (2023).
43. Seifi, S., Bakhtiari, M. A., Shaygani, H., Shamloo, A. & Almasi-Jaf, A. Investigating the correlation between the protein adhesion simulation and the biocompatibility of polymeric substrate for skin-tissue-engineering applications. *Phys. Chem. Chem. Phys.* **25**(15), 10697–10705. https://doi.org/10.1039/D2CP05763H (2023).
44. Shamloo, A. *et al.* Author correction: In-silico study of drug delivery to atherosclerosis in the human carotid artery using metal–organic frameworks based on adhesion of nanocarriers. *Sci. Rep.* **14**(1), 7868. https://doi.org/10.1038/s41598-024-58331-0 (2024).
45. Shaygani, H., Bakhtiari, M. A., Seifi, S., Mofrad, Y. M. & Shamloo, A. Investigating the surface gradient effects on the nano-machine's motion. *Comput. Mater. Sci.* **234**, 112774. https://doi.org/10.1016/j.commatsci.2023.112774 (2024).

Author contributions

M.A.B. designed and performed the simulations, analyzed the data, and wrote the paper. M.F. designed and performed the simulations, analyzed the data, and wrote the paper. F.A. analyzed the data, edited and wrote the paper. S.M.A.H designed and performed the simulations, analyzed the data, and wrote the paper. S.S. designed and performed the simulations, analyzed the data, and wrote the paper. P.H. designed and performed the simulations, analyzed the data, and wrote the paper. M.T.A. designed the simulations, analyzed the data, supervised the project and wrote the paper. A.A. designed the simulations, analyzed the data, supervised the project and wrote the paper.

Competing interests

The authors declare no competing interests.

Additional information

Supplementary Information The online version contains supplementary material available at https://doi.org/10.1038/s41598-024-69359-7.

Correspondence and requests for materials should be addressed to M.T.A.

Reprints and permissions information is available at www.nature.com/reprints.

Publisher's note Springer Nature remains neutral with regard to jurisdictional claims in published maps and institutional affiliations.